Susceptibility of Hermansky-Pudlak Mice to Bleomycin-Induced Type II Cell Apoptosis and Fibrosis

Lisa R. Young, Rajamouli Pasula, Peter M. Gulleman, Gail H. Deutsch, and Francis X. McCormack

Department of Medicine, Division of Pulmonary and Critical Care, University of Cincinnati; Department of Pediatrics, Division of Pulmonary Medicine, and Department of Pathology, Cincinnati Children's Hospital Medical Center, University of Cincinnati College of Medicine, Cincinnati, Ohio

Pulmonary inflammation, abnormalities in type II cell and macrophage morphology, and pulmonary fibrosis are features of Hermansky-Pudlak Syndrome (HPS), a recessive disorder associated with intracellular trafficking defects. We have previously reported that "Pearl" (*HPS2*) and "Pale Ear" (*HPS1*) mouse models have pulmonary inflammatory dysregulation and constitutive alveolar macrophage (AM) activation (Young LR *et al.*, *J Immunol* 2006;176:4361–4368). In the current study, we used these HPS models to investigate mechanisms of lung fibrosis. Unchallenged HPS1 and HPS2 mice have subtle airspace enlargement and foamy AMs, but little or no histologic evidence of lung fibrosis. Seven days after intratracheal bleomycin (0.025 units), HPS1 and HPS2 mice exhibited increased mortality and diffuse pulmonary fibrosis compared to strain-matched C57BL/6J wild-type (WT) mice. HPS mice had significantly increased collagen deposition, and reduced quasi-static and static compliance consistent with a restrictive defect. The early airway and parenchymal cellular inflammatory responses to bleomycin were similar in HPS2 and WT mice. Greater elevations in levels of TGF-β and IL-12p40 were produced in the lungs and AMs from bleomycin-challenged HPS mice than in WT mice. TUNEL staining revealed apoptosis of type II cells as early as 5 h after low-dose bleomycin challenge in HPS mice, suggesting that type II cell susceptibility to apoptosis may play a role in the fibrotic response. We conclude that the trafficking abnormalities in HPS promote alveolar apoptosis and pulmonary fibrosis in response to bleomycin challenge.

Keywords: alveolar type II cells; alveolar macrophage; lung fibrosis; Hermansky-Pudlak; adaptor protein 3

CLINICAL RELEVANCE

Hermansky-Pudlak Syndrome (HPS) is a highly penetrant genetic disorder of pulmonary fibrosis. This study demonstrates that bleomycin-challenged HPS mouse models have increased levels of TGF-β, early type II cell apoptosis, and marked pulmonary fibrosis.

Hermansky-Pudlak Syndrome (HPS) is a rare autosomal recessive disorder characterized by albinism, platelet dysfunction, and highly penetrant and frequently fatal pulmonary fibrosis (1, 2). There are currently eight genetic loci known to be associated with HPS in humans (3). Mutations in HPS genes result in defects in intracellular protein trafficking and in the biogenesis of lysosomes and lysosome-related organelles including melanosomes, platelet dense granules, and lamellar bodies in alveolar type II cells (4). Patients with HPS exhibit alveolar inflammation well before fibrosis is apparent, with accumulation of activated alveolar macrophages (AM) and elevated levels of proinflammatory cytokines and chemokines in bronchoalveolar lavage (BAL) fluid (5). Both the usual interstitial pneumonitis (UIP) pattern and cellular nonspecific interstitial pneumonitis (NSIP) pattern found in idiopathic pulmonary fibrosis (IPF) have been reported in HPS, but ceroid accumulations in alveolar macrophages, large hyperplastic alveolar type II cells with swelling and foamy degeneration, and lymphocytic and histiocytic infiltration of respiratory bronchioles are distinguishing features (6, 7). Clinically apparent pulmonary fibrosis develops in most individuals with HPS in the fourth or fifth decades of life (8). Potential contributions of environmental factors in HPS lung disease are not known, and it remains unclear how HPS trafficking abnormalities promote fibrosis.

Mouse models of HPS share many aspects of the human disease phenotype and provide the opportunity to investigate mechanisms of human disease from the vantage point of a known genetic defect. Ten of the currently available HPS mouse models, including the *HPS1* "Pale Ear" and *HPS2* "Pearl" mouse models used in this study, are naturally occurring and are maintained as congenic mutants on the C57BL/6J inbred strain. The gene product of *HPS2* in Pearl mice and humans with HPS2 is the β3A subunit of the adaptor protein-3 (AP-3) complex, a heterooligomer of four subunits (μ3a, σ3, δ, and β3) that functions in organelle biogenesis and protein trafficking (9). Mutations in individual AP-3 subunits result in instability and ubiquitin-mediated degradation of the entire AP-3 complex, which leads to abnormalities in intracellular trafficking in a variety of cell types and organ systems. The "Pale Ear" *HPS1* mouse is the model for the most common HPS subtype, and although the precise function of the *HPS1* gene product (HPS1) remains unknown, it is also clearly critical for intracellular protein trafficking.

Other human diseases provide evidence that abnormal protein trafficking in type II cells can cause interstitial lung disease (ILD) (10, 11). Mutations in surfactant protein C (SP-C) cause SP-C protein misfolding and activation of endoplasmic reticulum (ER) stress pathways (12), and the adaptation to the chronic ER stress is associated with an increased susceptibility to RSV-induced death of type II cells (13). Mutations in the ATP-binding cassette family member of proteins, *ABCA-3* gene, affect lipid transport into lamellar bodies, and also cause ILD through type II cell–dependent mechanisms (14, 15). Apoptosis of alveolar type II cells is also a prominent feature of many types of ILD, and correlates with disease progression in IPF and extent of fibrosis in animal models (16, 17).

(*Received in original form December 20, 2006 and in final form February 27, 2007*)

This work was funded by an American Thoracic Society/Hermansky-Pudlak Syndrome Network grant (L.R.Y.), a Procter Scholar Award (L.R.Y.), HL68861 (F.X.M.), and by the Department of Veterans Affairs (F.X.M.).

Correspondence and requests for reprints should be addressed to Francis X. McCormack, M.D., University of Cincinnati, Pulmonary, Critical Care, and Sleep Medicine, 231 Albert Sabin Way ML 0564, Cincinnati, OH 45267. E-mail: frank.mccormack@uc.edu

Originally Published in Press as DOI: 10.1165/rcmb.2006-0469OC on March 15, 2007
Internet address: www.atsjournals.org

Pearl and Pale Ear HPS mice have been shown to have structural abnormalities in the alveolar compartment that are similar to those observed in humans with HPS, including foamy AMs and enlarged type II cells containing irregular dense inclusions (6, 18), and expansion of interstitial septa by excess collagen fibrils at the ultrastructural level (18). Others have shown that double-mutant HPS1/HPS2 (*ep/pe*) mice have impaired lamellar body secretion from type II cells (19), and that lung hydroxyproline content is significantly increased compared with controls (20). Furthermore, silica-challenged Pale Ear mice develop a persistent accumulation of activated macrophages and increased collagen fibers in alveolar tissues (21). However, unchallenged Pearl and Pale Ear mice do not spontaneously develop histologically significant pulmonary fibrosis by 1 yr of age, but instead exhibit progressive airspace enlargement (20). Therefore, whether the phenotype of HPS mouse models includes susceptibility to pulmonary fibrosis has remained controversial.

We have previously demonstrated that Pearl and Pale Ear mice have basal inflammatory dysregulation and constitutive AM activation that parallels abnormalities reported in patients with HPS (5, 22). We wondered whether HPS mice would develop enhanced fibrosis in response to inhalation challenge with bleomycin. Bleomycin is a chemotherapeutic agent known to induce the release of cytokines, augment fibroblast proliferation and activity, and to cause human and animal lung parenchymal injury and subsequent lung fibrosis. Therefore, we investigated the responses of HPS mice to intratracheal bleomycin challenge.

MATERIALS AND METHODS

Mice

Breeding pairs of Pearl (HPS2 mutation) and Pale Ear (HPS1 mutation) mice that had been maintained on the C57BL/6J background were gifts from Dr. R. Swank (Roswell Park Cancer Institute, Buffalo, NY). C57BL/6J mice (Jackson, Bar Harbor, ME) were used as the wild-type (WT) control for comparisons with HPS mice. Mice were housed in a barrier facility and studied using procedures approved by the University of Cincinnati Institutional Animal Care and Use Committee. Sentinel mice that were tested periodically were free of known viral and bacterial pathogens. Male mice, age 8–14 wk, were used for all studies.

Bleomycin Challenge

Mice were anesthetized to moderate depth with isofluorane (Forane; Ohmeda Caribe, Guyama, Puerto Rico). After topical sterilization with ethanol, the trachea was minimally exposed via a ventral midline neck incision and cannulated with a sterile catheter. Bleomycin sulfate (0.025–0.05 U/mouse; Sigma, St. Louis. MO) or saline control was instilled intratracheally, the incision was closed with surgical adhesive, and the mice were observed through recovery.

Lung Histology and Immunohistochemistry

Animals were killed by pentobarbital injection, and 0.9 ml of 10% buffered formalin was instilled into the lungs via a tracheal cannula at 25 cm H_2O. Lung tissues were paraffin embedded and cut into 5-μm sections by conventional methods. Slides were stained with hematoxylin and eosin (H&E) or trichrome blue. Endogenous peroxidase activity was blocked with immersion of deparaffinized sections in 3% H_2O_2 for 10 min. For antigen retrieval, the sections were placed in 0.1 M citrate buffer, pH 6.0, and treated with microwave for 10 min. Type II cells were identified using a rabbit polyclonal antibody against human pro-SP-C (kind gift of J. Whitsett, M.D., Cincinnati Children's Hospital Medical Center, Cincinnati, OH) (dilution 1:1500) and the Vectastain ABC System (Vector Labs, Burlingame, CA) with DAB or NovaRED (according to the manufacturer's instructions). Immunostains were performed with active caspase 3 goat polyclonal IgG (sc-1226, 1:50 dilution; Santa Cruz Biotechnology, Santa Cruz, CA) using a similar protocol. Sections were then lightly counterstained with hematoxylin.

Lung Physiology

Mice were anesthetized and tracheostomized, and respiratory mechanics were measured using forced oscillation technique (0.25–20 Hz) (Flexivent; SCIREQ, Montreal, PQ, Canada). Estimated total lung compliance, airway resistance and elastance, and tissue damping were obtained by fitting a model to each impedance spectrum.

Quantitation of Lung Collagen Content

Whole lungs were harvested, weighed, snap-frozen, and stored at −80°C. Total soluble collagen was measured using the Sircol assay (Biocolor; Accurate Chemical And Scientific Corporation, Westburg, NY) according to the manufacturer's instructions. Briefly, lungs were homogenized in PBS, and Sircol dye was incubated with test samples or collagen standard on a rocker for 30 min. Samples were then centrifuged, unbound dye solution was removed, and the remaining collagen-bound dye pellet was solubilized. Absorbance was measured at 540 nm and compared with a calibration curve generated using the collagen standard provided by the manufacturer.

Evaluation of Airway and Tissue Cellular Recruitment

Mice were killed by lethal pentobarbital injection followed by transection of the abdominal aorta. BAL was performed as described, after tracheostomy and intubation with a sterile 20-gauge adapter, by gentle instillation and aspiration of three 1-ml aliquots of 0.9% saline with 5 mM Tris. After separation of the BAL cells by low-speed centrifugation (450 × g, 10 min, 4°C), the cell-free BAL fluid was stored at −80°C until use. Cells were resuspended in PBS and counted using a Coulter counter or hemacytometer. A cell aliquot was spun onto glass slides using a cytocentrifuge (speed 300, 5 min; Shandon, Thermo Fisher Scientific, Ontario, Canada), and cytospin preparations were stained with DiffQuik (Sigma-Aldrich, St. Louis, MO). The percentages of macrophages, neutrophils, lymphocytes, and eosinophils in BAL were determined by differential counting of a minimum of 200 cells.

For analysis of tissue cellular composition, organs were individually harvested in Hanks' Buffered Salt Solution (HBSS) and teased apart between glass slides. A cell suspension was obtained by aspiration through a 21.5-ga. needle and filtering with 60-μm nylon mesh (Spectrum Laboratories, Inc., Rancho Dominguez, CA). The cell pellet was collected by centrifugation (450 × g, 5 min, 4°C) and resuspended in HBSS. The lymphocyte population was then isolated using a 40–70% Percoll (Pharmacia, Uppsala, Sweden) gradient (23). Cells were incubated with allophyocyanin (APC) or fluorescein isothiocyanate–conjugated antibodies (1 μg antibody per 20 μl staining buffer) and isotype controls. Antibodies used to tag specific cell types included anti-F4/80 for macrophages (CalTag, Carlsbad, CA), anti-GR1 for neutrophils, and anti-CD3 for lymphocytes (BD Biosciences, Bedford, MA). Cells were fixed in 1% paraformaldehyde in PBS and stored at 4°C before analysis on a FACS Calibur (Becton Dickinson, San Jose, CA). Data were analyzed using FCS Express 2.0 software (De Novo Software, Thornhill, ON, Canada).

Enzyme-Linked Immunosorbent Assay Measurements of Cytokines and Chemokines

Cytokine protein concentrations in cell-free BAL, lung homogenate, and AM cell culture media supernatant were quantified by ELISA (murine Quantikine kits; R&D Systems, Minneapolis, MN), using the chromogenic substrate tetramethylbenzidine and analysis with a microtiter plate spectrophotometer at a wavelength of 450 nm.

Evaluation of Apoptosis

Terminal deoxynucleotidyl transferase-mediated dUTP nick end labeling (TUNEL) was performed on deparaffinized lung tissue sections using the In Situ Cell Death detection kit (Roche Diagnostics, Mannheim, Germany) according to the manufacturer's instructions. After permeabilization, tissue sections were incubated in TUNEL reaction mixture (or the labeling solution without addition of TdT enzyme as a negative control) for 1 h at 37°C. Fluorescence images were visualized and collected with a digital camera mounted on an Olympus BX60 fluorescence microscope (Olympus America, Center Valley, PA), and analyzed using SPOT RT Software v3.4 (SPOT Diagnostic, Sterling Heights, MI). For immunofluorescent double-staining of alveolar type

II cells and TUNEL, type II cells were identified by a rabbit polyclonal antibody against human pro–SP-C (dilution 1:1,000), biotinylated anti-rabbit IgG secondary antibody (dilution 1:1,000), and detection with Cy3 red (dilution 1:3,000), immediately followed by TUNEL procedure as above. For quantitative evaluation of TUNEL staining, the mean number of cells with TUNEL-positive nuclei and pro–SP-C–positive cells were recorded by two independent observers (L.R.Y. and P.M.G.) from 10 sequential, nonoverlapping high-power fields from each specimen and expressed as a ratio.

Statistical Analysis

Numeric data are presented as mean ± SEM. Parametric data were evaluated using the Student's *t* test, or by one-way ANOVA for comparison of more than two groups (Prism 4; Graph Pad Software, Inc., San Diego, CA). The log rank test was used for survival analysis. *P* values < 0.05 were considered significant.

RESULTS

Pearl Mice Have Increased Mortality When Exposed to Intratracheal Bleomycin

Pearl mice were challenged with intratracheal bleomycin (or saline control) at doses (0.025 and 0.05 U/mouse in volume of 50 μl) that are considered sub-lethal for this mouse strain (24, 25). As shown in Figure 1, bleomycin challenge led to significantly greater mortality in Pearl than WT mice. Bleomycin at a dose of 0.05 U/mouse resulted in 100% mortality in Pearl mice after 7 d (Figure 1B, $P < 0.001$ by log-rank test), while a reduced dose of 0.025 U/mouse resulted in 50% mortality in Pearl mice at Day 10 and only 8% mortality in WT mice (Figure 1A, $P < 0.001$). No deaths occurred in Pearl or WT mice receiving intratracheal saline as controls. Significantly greater weight loss occurred in Pearl than WT mice by Day 7 after intratracheal bleomycin challenge (not shown). Based on these dose–response data, all further bleomycin experiments were performed with the lower dose of 0.025 U. Mortality for Pale Ear mice was 14% within 7 d after intratracheal bleomycin challenge of 0.025 U.

HPS Mice Have Increased Fibrotic Susceptibility to Bleomycin Challenge

Significant histologic differences were observed in the lungs of HPS and WT mice 7 d after intratracheal bleomycin. In WT mice, very limited cellular inflammation and histologic evidence of fibrosis was apparent, while Pearl and Pale Ear mice developed marked fibrosis with a varying extent of cellular interstitial expansion (Figure 2). When challenged with 0.025 U of bleomycin, histologic fibrosis did not become evident in WT mice until after 14 d (not shown). The extent of fibrosis, as measured by a colorimetric assay (Sircol red) of total lung collagen content, was significantly greater in the lungs of Pearl and Pale Ear than WT mice (Figure 3).

Pearl Mice Have Reduced Lung Compliance after Bleomycin Challenge

In order to determine if the observed histologic changes were associated with significant physiologic impairment, a forced oscillation technique was used to assess pulmonary compliance in Pearl mice. While no significant physiologic changes were detected in bleomycin-treated WT mice at the 7-d point, quasi-static and static compliance were significantly decreased in bleomycin-challenged Pearl mice (0.046 ± 0.003 ml/cm H_2O for Pearl versus 0.066 ± 0.006 ml/cm H_2O for WT, $P < 0.05$) after 1 wk (Figure 4).

Airway and Pulmonary Inflammatory Cell Recruitment in Pearl Mice Is Similar to That in WT Mice after Intratracheal Bleomycin Challenge

Intratracheal bleomycin challenge is associated with a robust early cellular inflammatory response (25, 26). We have previously reported that total BAL cell numbers and differentials are not significantly different at baseline in Pearl, Pale Ear, and WT mice (22). After intratracheal bleomycin challenge, total BAL cell numbers were increased, and cell differentials were similar in Pearl and WT mice at 1 and 3 d (Figures 5A and 5B). Both WT and Pearl mice had a neutrophil-rich cellular influx that peaked at approximately Day 3. Lymphocytes were also recruited to the airspace. A modest influx of eosinophils also occurred in both WT and Pearl mice (not shown). Using FACS analysis, total lung leukocyte cell numbers and proportions of neutrophils, macrophages, and lymphocytes were found to be similar in Pearl and WT mice 3 d after intratracheal bleomycin (not shown).

HPS Mice Have Elevated Levels of Profibrotic Mediators after Bleomycin Challenge

Bleomycin-induced fibrosis in animal models has been shown to be associated with production of profibrotic mediators including TGF-β1 and IL-12 (27, 28). While the level of TGF-β1 was similar in the pulmonary tissues of unchallenged Pearl, Pale Ear, and WT mice, elevated levels of activated TGF-β1 were present in the lungs of HPS mice after bleomycin challenge (Figure 6A). This difference was not statistically significant until 3 d after bleomycin challenge (4,215 ± 1,081 pg/ml for Pearl versus 2,792 ± 805 pg/ml for WT, $P < 0.05$). Higher levels of activated TGF-β1 were also present in the lungs of Pale Ear mice 7 d after bleomycin challenge (15,340 ± 1,118 pg/ml for Pale Ear versus 5,278 ± 1,072 pg/ml for WT, $P < 0.05$). IL-12/23p40 concentrations were significantly elevated in the lungs of unchallenged Pearl versus WT mice (563 ± 61 pg/ml for Pearl versus 288 ± 32 pg/ml for WT, $P < 0.05$), and bleomycin challenge resulted in further time-dependent increases in the lungs of Pearl mice (Figure 6B). Levels of IL-12/23p40 were also greater in the lungs of Pale Ear compared with WT mice, both at baseline

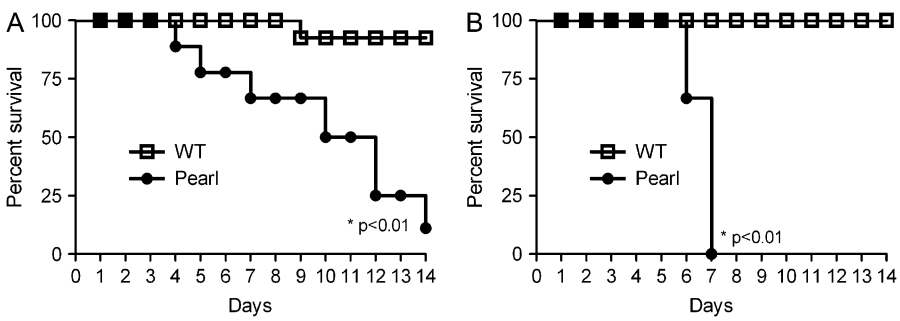

Figure 1. Survival rate of Pearl and WT mice after intratracheal bleomycin. WT (*open squares*) and Pearl (*circles*) mice were challenged by intratracheal instillation of a single bleomycin dose (0.025 U/mouse in *A* or 0.05 U/mouse in *B*). Mortality was monitored over 2 wk ($n = 12$ per group for 0.025 U and $n = 8$ per group for 0.05 U).

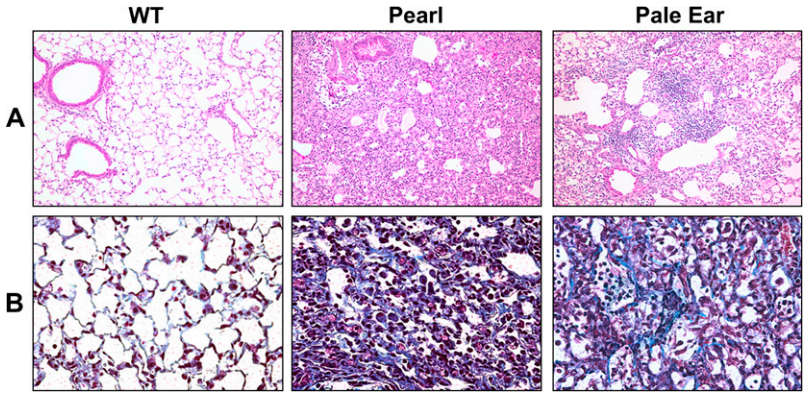

Figure 2. Increased evidence of pulmonary fibrosis in HPS versus WT mice after bleomycin challenge. Mice were challenged with intratracheal bleomycin (0.025 U). After 7 d, lungs were inflation-fixed with 10% buffered formalin at 25 cm H_2O. Representative low-power (×10) (*A*) and high-power (×40) (*B*) photomicrographs are shown for WT, Pearl, and Pale Ear bleomycin-treated mice ($n = 4$ per group). Histologic analysis was performed with H&E staining (*A*) and Masson's trichrome staining to localize collagen fibers (*B*).

(not shown) and 7 d after intratracheal bleomycin challenge (1,820 ± 360 pg/ml for Pale Ear versus 1,086 ± 128 pg/ml for WT, $P < 0.05$). AMs isolated from bleomycin-challenged Pearl and Pale Ear mice demonstrated more than 2-fold greater production of TGF-β1 compared to WT AMs over a 24-h incubation period in culture (Figure 6C). As we have previously reported, unchallenged HPS AMs constitutively produce elevated levels of IL-12/23p40 (22). Bleomycin challenge *in vivo* also led to greater IL-12/23p40 production from AMs isolated from HPS mice than from WT mice (Figure 6D). In contrast to the findings for the profibrotic mediators TGF-β and IL-12/23p40, levels of IL-12p70, IL-1β, TNF-α, and MIP1α were similar in BAL fluid and lung tissue from Pearl and WT mice after bleomycin challenge (not shown).

Apoptosis Is Increased in the Lungs of HPS Mice after Bleomycin Challenge

To investigate mechanisms of the fibrotic susceptibility in HPS mice, TUNEL assay was used to screen for apoptosis in pulmonary cells after low dose intratracheal bleomycin challenge. Limited evidence of apoptosis was apparent in the lungs of unchallenged Pearl and Pale Ear mice and in the lungs of WT mice up to 7 d after bleomycin instillation (0.025 U) (not shown). In contrast, increased apoptosis was detected in lung sections from Pearl and Pale Ear mice as early as 5 h after intratracheal bleomycin challenge (Figures 7A–7C). Co-immunostaining for pro–SP-C was used to identify TUNEL-positive cells as alveolar type II cells (Figures 7D–7F), and the ratio of TUNEL-positive to SP-C–positive cells was quantitated from 10 consecutive ×40 microscopic fields from each of three animals at each timepoint and group (Figure 7I). Positive immunostaining for active caspase 3 was rarely seen in lung sections from HPS or WT mice at baseline or Day 1 (not shown), but was more abundant in the lungs of Pearl and Pale Ear than WT mice starting 3 d after bleomycin challenge (Figures 7G and 7H).

We have previously reported that increased levels of soluble Fas are present in BAL fluid from unchallenged Pearl mice (22), and therefore investigated whether abnormalities in the Fas/FasL system might be responsible for enhanced apoptosis of Pearl type II cells via an extrinsic apoptotic pathway. ELISA of lung homogenates and BAL revealed similarly elevated levels of soluble Fas ligand (FasL) in the lungs of Pearl and WT mice at Days 1 and 3 after bleomycin challenge. It was not until Day 7 after bleomycin challenge that significantly greater levels of FasL were present in the lungs of Pearl versus WT mice (Figure 7H). Furthermore, immunohistochemistry for Fas receptor and Fas ligand at baseline and at Days 1 and 3 revealed no detectable differences in extent or distribution of expression between Pearl and WT mice (not shown).

DISCUSSION

These experiments provide a comprehensive assessment of the response of Pearl mice to bleomycin challenge and demonstrate that Pearl and Pale Ear HPS mouse models have a pulmonary phenotype that includes fibrotic susceptibility. Although C57BL/6J is a mouse strain known for susceptibility to bleomycin-induced fibrosis (25, 29), the WT animals were only modestly affected at the 7-d timepoint by the bleomycin doses that induced diffuse fibrosis and mortality in strain-matched HPS mice. Bleomycin-challenged HPS mice also exhibited increased weight

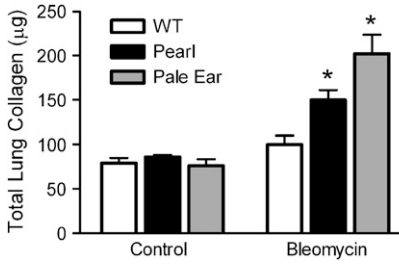

Figure 3. Increased collagen deposition in HPS lungs in response to bleomycin challenge. Mice were challenged with intratracheal bleomycin (0.025 U) or an equal volume of sterile saline as a control. After 7 d, lungs were harvested and levels of total lung collagen were assayed using the colorimetric Sircol assay. (Values indicate totals for both lungs from each mouse; $n = 8$ per group for WT, $n = 4$ per group for Pearl and Pale Ear, $^*P < 0.01$.)

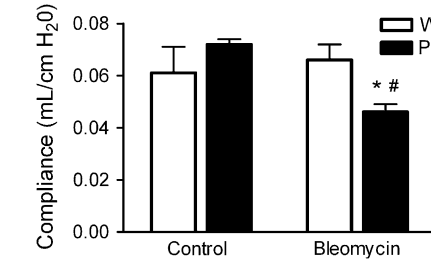

Figure 4. Reduced quasi-static pulmonary compliance in Pearl mice after bleomycin challenge. Mice were challenged with intratracheal bleomycin (0.025 U) or an equal volume of sterile saline as a control. After 7 d, tracheostomized mice underwent physiologic testing with the Scireq flexivent system ($n = 4$ per group, $^*P < 0.05$ for WT versus Pearl bleomycin and $^{\#}P < 0.01$ for Pearl control versus Pearl bleomycin). *Open bars*, wild type; *solid bars*, Pearl.

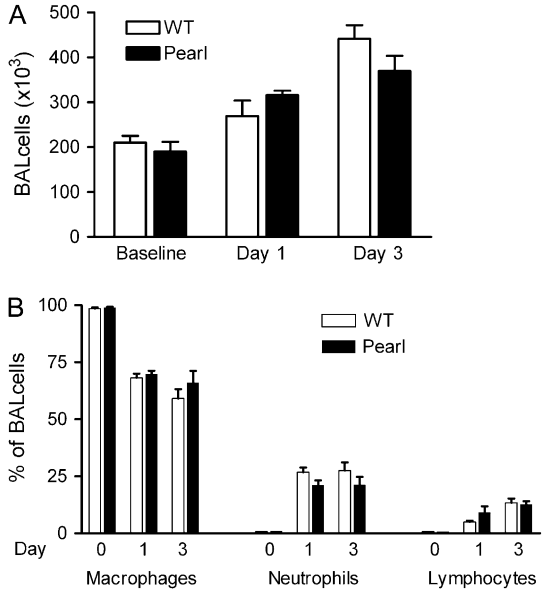

Figure 5. BAL cell populations after bleomycin challenge. Mice were challenged with intratracheal bleomycin (0.025 U), and BAL was performed at various time points as indicated. (*A*) Total BAL cell counts at baseline, and Days 1 and 3 after bleomycin challenge (P = ns for Pearl versus WT at each time point). (*B*) BAL cell differentials at baseline and days 1 and 3 after bleomycin challenge (P = ns for Pearl versus WT for all comparisons). *Open bars*, WT; *solid bars*, Pearl.

loss, histologic evidence of fibrosis, and biochemical evidence of collagen deposition compared with strain-matched WT mice. These findings in Pearl mice were associated with reduced pulmonary compliance consistent with a restrictive physiologic defect. These data support the use of HPS mice as models of pulmonary fibrosis.

HPS ranks among the most penetrant genetic disorders of pulmonary fibrosis in adults, as virtually all patients with HPS who survive to adulthood develop fibrotic lung disease (1, 30). HPS1 is the most common human genotype, and accounts for the majority of ILD cases reported in HPS. Although the eight reported HPS2 patients are younger in age than HPS1 and HPS4 patients with pulmonary fibrosis, mild pulmonary fibrosis was described in two HPS2 cases (31, 32). In this study, key findings of bleomycin-induced histologic fibrosis and alveolar type II cell apoptosis in the *HPS2* mice were also confirmed in Pale Ear *HPS1* mice, the more common genetic background associated with fibrosis.

The role of cellular inflammation in ILD pathogenesis remains unclear. While idiopathic pulmonary fibrosis (IPF) is increasingly recognized as a pauci-immune disorder with fibroblastic proliferation but relatively minimal leukocyte infiltration, robust cellular interstitial inflammation precedes fibrosis in multiple other forms of ILD such as hypersensitivity pneumonitis, sarcoidosis, desquamative interstitial pneumonitis, respiratory bronchiolitis, and ILD associated with mutations in SP-C and connective tissue disease (33–35). Alveolar inflammation also precedes pulmonary fibrosis in patients with HPS (5), but the direct role of inflammation in the pathogenesis of HPS lung disease has not been determined. We have previously reported that Pearl and Pale Ear mice exhibit pulmonary inflammatory dysregulation, with constitutive AM activation and exaggerated cytokine responses to endotoxin challenge (22). In the bleomycin model of pulmonary fibrosis, inflammation induces the release of cytokines that promote fibroblast proliferation and production of extracellular matrix (26, 36). In this context, we postulated that Pearl mice would have an aberrant early and exaggerated inflammatory response to bleomycin challenge. However, similar elevations in selected pro-inflammatory cytokines and chemokines, and in early airway and parenchymal cellular inflammatory recruitment, occurred in Pearl and WT mice after bleomycin challenge. Further studies are needed to determine whether pulmonary inflammation and fibrosis are causally linked in HPS.

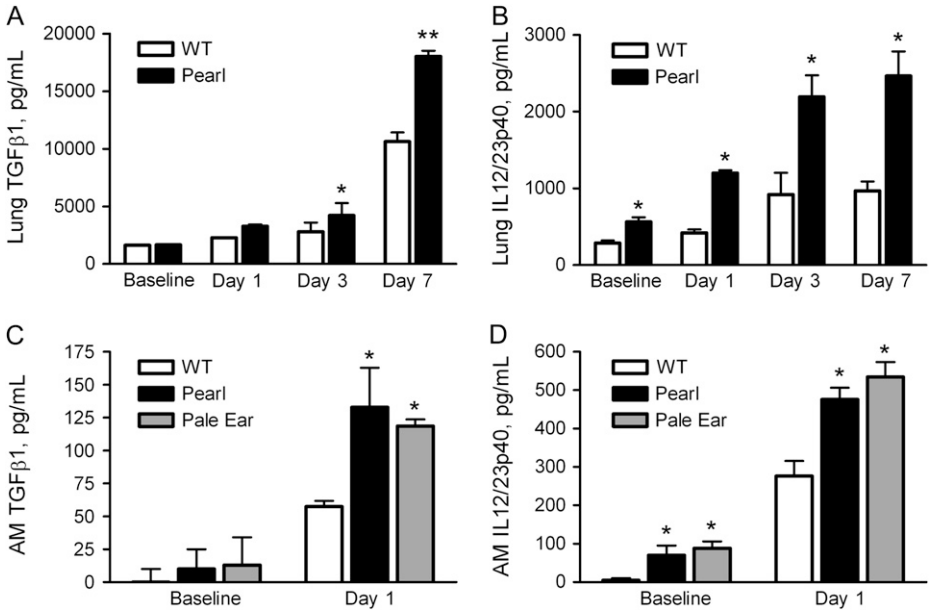

Figure 6. Elevated TGF-β and IL-12p40 levels in Pearl mice after bleomycin challenge. (*A*) TGF-β1 levels in the lungs of Pearl mice at baseline and after bleomycin challenge. Mice were challenged with intratracheal bleomycin (0.025 U). After 0, 1, 3, or 7 d, lungs were harvested and homogenized. Acid-activated TGF-β1 was measured by ELISA (n = 4 per group, $^*P < 0.05$ for WT versus Pearl at Day 3, $^{**}P < 0.001$ for WT versus Pearl at Day 7). (*B*) IL-12/23p40 levels in the lungs of Pearl mice at baseline and after bleomycin challenge. Mice were challenged with intratracheal bleomycin (0.025 U) and levels of IL-12/23p40 in lung homogenate were measured by ELISA (n = 4 per group, $^*P < 0.05$ for WT versus Pearl at all time points). (*C*) TGF-β1 production from AM after bleomycin challenge *in vivo*. AMs were isolated from Pearl, Pale Ear, and WT mice at baseline and 24 h after bleomycin challenge. Acid-activated TGF-β1 was measured from the cell media supernatant after 24 h in culture (n = 5 per group for WT, n = 3 per group for Pearl and Pale Ear, $^*P < 0.05$ for Pearl and Pale Ear versus WT). (*D*) IL-12/23p40 production from AMs after bleomycin challenge *in vivo*. AMs were isolated from Pearl, Pale Ear, and WT mice at baseline and 24 h after bleomycin challenge. IL-12/23p40 was measured from the cell media supernatant after 24 h in culture (n = 5 per group for WT, n = 3 per group for Pearl and Pale Ear, $^*P < 0.05$ for Pearl and Pale Ear versus WT). *Open bars*, WT; *solid bars*, Pearl; *shaded bars*, Pale Ear.

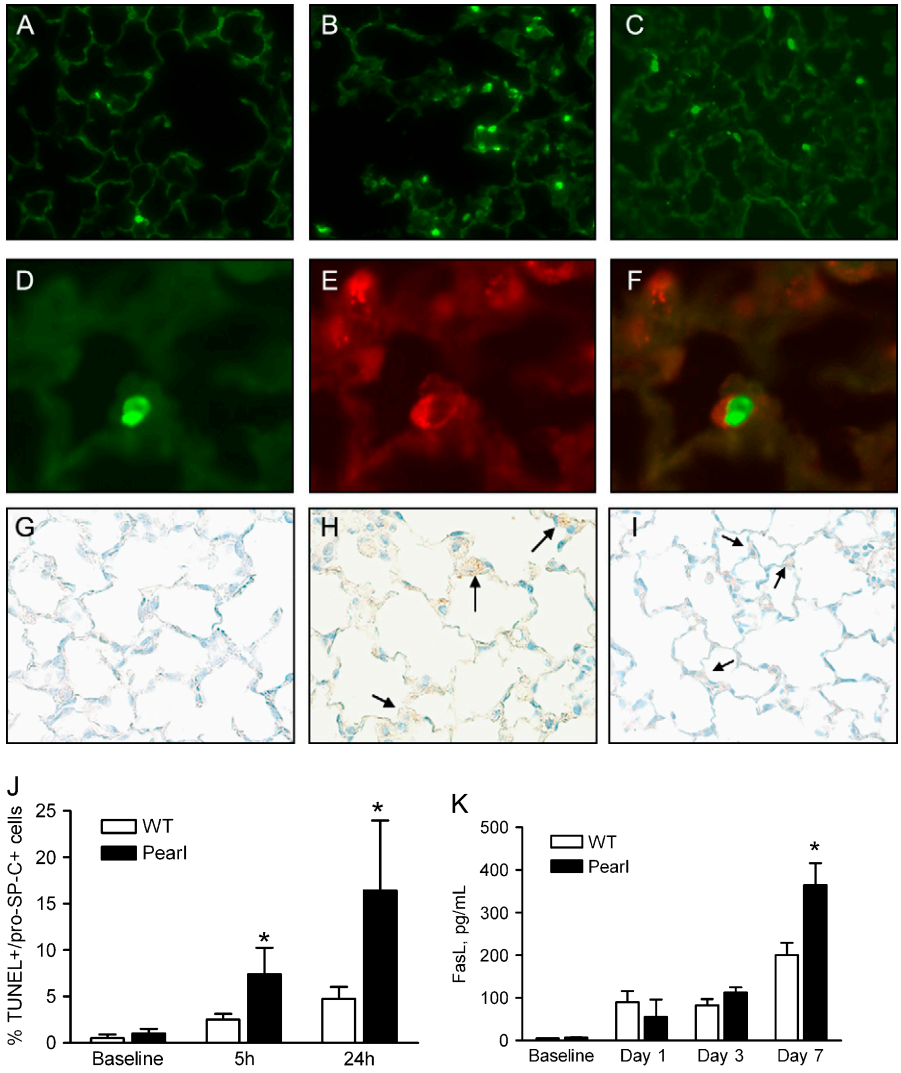

Figure 7. Increased apoptosis in lung sections from HPS mice after intratracheal bleomycin challenge. At indicated time points after intratracheal bleomycin (0.025 U), lungs were inflation-fixed in formalin as previously described. TUNEL assay (Roche) was performed on paraffin-embedded sections. (*A*–*C*) Representative fluorescent micrographs (×40) for (*A*) WT, (*B*) Pearl, and (*C*) Pale Ear at 5 h after bleomycin challenge are shown. (*D*–*F*) Representative co-immunofluorescence for TUNEL (*D*) and pro–SP-C (*E*) identifies apoptotic alveolar type II cells (*F*, merge) from a Pearl lung section, 5 h after intratracheal bleomycin challenge. (*G* and *H*) Representative photomicrographs (×40) of active caspase 3 staining in lung sections from (*G*) WT, (*H*) Pearl, or (*I*) Pale Ear mice, 3 d after intratracheal bleomycin challenge. Increased numbers of cells positive for active caspase 3 were present in the lungs of Pearl and Pale mice. *Arrows* indicate examples of positive cells. (*J*) Quantitative assessment of percentage of alveolar type II cells which are TUNEL-positive. Alveolar wall TUNEL-positive and SP-C–positive cells were counted from 10 high-power (×40) fields ($n = 3$ each at baseline and 5 h, $n = 4$ each at 24 h, $^*P < 0.05$). (*K*) Levels of Fas ligand in the lungs of Pearl mice after intratracheal bleomycin challenge. Mice were challenged with intratracheal bleomycin (0.025 U). Mice were killed at various time points, lungs were harvested, and Fas ligand (FasL) levels were assessed by ELISA ($n = 4$ per group, $^*P < 0.05$ for Pearl versus WT, Day 7).

Profibrotic cytokines such as TGF-β cause fibroblast transformation and proliferation, leading to deposition of extracellular matrix (37, 38), and multiple studies have demonstrated that TGF-β is a key factor in fibrosis in the lung and in other tissues. In animal models, adenoviral-driven overexpression of TGF-β1 results in pulmonary fibrosis, and blocking the action of TGF-β attenuates fibrosis (28, 37, 39). Our studies revealed greater elevations in levels of TGF-β in the lungs of bleomycin-challenged HPS than WT mice. Further, isolated murine HPS AMs produced excess quantities of TGF-β compared with WT AMs after bleomycin challenge. In addition, IL-12/23p40, but not IL-12p70, was constitutively produced by HPS AMs and found in elevated levels in the lungs of HPS versus WT mice, both at baseline and after bleomycin challenge. Previous studies have demonstrated that the profibrotic IL-12p40 subunit, but not the IL-12p70 heterodimer, is overproduced during experimental induction of fibrosis, and that AMs are the predominant source (40). Further, IL-12p40−/− mice are resistant to silica-induced fibrosis (41), and a monoclonal antibody to IL12 was protective in the bleomycin model (27). Together, our findings of increased IL-12p40 and TGF-β production from HPS AMs suggest a possible link between macrophage dysfunction and fibrogenesis in HPS.

In addition to cytokine/chemokine imbalance, many studies support the concept that alveolar epithelial cell apoptosis is a dominant feature of human fibrotic lung disease and pulmonary fibrosis in the bleomycin model (42). In lung biopsies from patients with IPF, alveolar epithelial cell apoptosis has been found in regions adjacent to myofibroblasic proliferation and collagen deposition (16, 43). Among the fibrogenic factors we assessed, the earliest distinguishing finding between HPS and WT mice after bleomycin challenge was apoptosis of type II cells. TUNEL staining revealed apoptosis of alveolar type II cells as early as 5 h after bleomycin challenge in HPS mice, and the subsequent increase in caspase-3 activation indicates that the initial DNA fragmentation and cellular injury was followed by apoptotic cell death. Our data suggest that type II cell susceptibility to apoptosis may play a role in the fibrotic response, although the absolute extent of type II cell apoptosis required to induce fibrosis is not known. Bleomycin challenge induced increased levels of TGF-β1 in HPS mice, and TGF-β1 has been shown to enhance Fas-mediated epithelial cell apoptosis and pulmonary fibrosis (44). However, our data would suggest that TGF-β is not the sole contributor to Pearl type II cell apoptosis and fibrosis, as apoptosis, which occurred as early as 5 h after bleomycin challenge, preceded a detectable increase in TGF-β levels *in vivo*.

Apoptosis occurs via an extrinsic pathway in response to activation of cell membrane receptors as well as via an intrinsic pathway triggered by release of mitochondrial products. The extrinsic pathway is mediated by the death receptor family, which includes TNF receptor and the Fas receptor (CD95). The Fas

receptor can be activated by either Fas ligand (FasL) on the surface of cytotoxic lymphocytes, or by a soluble form of FasL (sFasL) (45). Mice deficient in Fas are protected from bleomycin-induced fibrosis, and administration of a soluble Fas antigen or an anti-Fas ligand antibody prevents bleomycin-induced epithelial apoptosis and pulmonary fibrosis (46), as do caspase inhibitors (47). Furthermore, experimental induction of apoptosis in mice via inhalation of anti-Fas antibody has been shown to result in pulmonary fibrosis (48).

We have previously reported that Pearl mice have increased basal pulmonary levels of sFas (22). Based on knowledge that FasL is a member of the TNF family, which is expressed predominantly in the lytic granule of activated T lymphocytes and natural killer cells (49), and that AP-3 has previously been shown to be critical for the movement of T-cell lytic granules to the immunological synapse (50), we hypothesized that AP-3 deficiency in Pearl mice would lead to abnormalities in the Fas/FasL system that would promote apoptosis via an extrinsic pathway. However, we found no baseline differences in expression of Fas receptor or FasL by ELISA or immunohistochemistry. While levels of FasL were elevated in Pearl mice as compared to WT mice, the difference did not occur until 7 d after bleomycin challenge, the time point at which fibrosis was already evident.

An intrinsic apoptotic mechanism is perhaps more likely in HPS-affected cells. The finding that alveolar apoptosis is increased in both *HPS2* and *HPS1* mice suggests a common, mistrafficking-mediated mechanism of apoptotic susceptibility that is not genotype-specific. SP-C misfolding mutations are associated with marked phenotypic variability with respect to penetrance, age of onset, and disease severity (10, 11). Evidence of ER stress (13) and susceptibility to bleomycin-induced apoptosis and fibrosis from SP-C models (17) suggests that environmental insults, which overwhelm the homeostatic activities of marginally compensated type II cells, may provide a "second hit" which leads to fibrosis. Future studies are planned to investigate mechanisms of HPS type II cell apoptotic susceptibility.

Although many animal models of pulmonary fibrosis exist, the bleomycin model is one of the most widely studied. Bleomycin is associated with a myriad of injurious effects, and numerous mechanisms have been postulated to influence the outcome of bleomycin challenge. This study identifies HPS mice as a promising and experimentally tractable model to examine the molecular basis of pulmonary fibrosis using genetic and cellular replacement techniques.

In summary, we conclude that HPS mice exhibit susceptibility to bleomycin-induced alveolar type II cell apoptosis, pulmonary fibrosis, and mortality. Cellular and molecular insights into the pathogenesis of HPS lung disease may enhance the understanding and therapeutic approach to more common fibrotic lung disorders.

Conflict of Interest Statement: None of the authors has a financial relationship with a commercial entity that has an interest in the subject of this manuscript.

Acknowledgments: The authors thank Dr. Richard Swank for providing the Pearl and Pale Ear mice. They thank Dr. William J. Martin, II for guidance in design of bleomycin studies, Camille Kapita for technical assistance with intratracheal challenges, and Dr. Ping Wang for assistance with measurement of murine lung physiology.

References

1. Brantly M, Avila NA, Shotelersuk V, Lucero C, Huizing M, Gahl WA. Pulmonary function and high-resolution CT findings in patients with an inherited form of pulmonary fibrosis, Hermansky-Pudlak syndrome, due to mutations in HPS-1. *Chest* 2000;117:129–136.
2. Gahl WA, Brantly M, Kaiser-Kupfer MI, Iwata F, Hazelwood S, Shotelersuk V, Duffy LF, Kuehl EM, Troendle J, Bernardini I. Genetic defects and clinical characteristics of patients with a form of oculocutaneous albinism (Hermansky-Pudlak syndrome). *N Engl J Med* 1998;338: 1258–1264.
3. Morgan NV, Pasha S, Johnson CA, Ainsworth JR, Eady RA, Dawood B, McKeown C, Trembath RC, Wilde J, Watson SP, *et al.* A germline mutation in BLOC1S3/reduced pigmentation causes a novel variant of Hermansky-Pudlak syndrome (HPS8). *Am J Hum Genet* 2006;78: 160–166.
4. Li W, Rusiniak ME, Chintala S, Gautam R, Novak EK, Swank RT. Murine Hermansky-Pudlak syndrome genes: regulators of lysosome-related organelles. *Bioessays* 2004;26:616–628.
5. Rouhani F, Gahl WA, Tobias C, Jolley C, Brantly M. Cellular and cytokine characteristics of epithelial lining fluid in individuals with pulmonary fibrosis who harbor a 16-bp duplication in the Hermansky-Pudlak syndrome gene [abstract]. *Am J Respir Crit Care Med* 2000; A503.
6. Nakatani Y, Nakamura N, Sano J, Inayama Y, Kawano N, Yamanaka S, Miyagi Y, Nagashima Y, Ohbayashi C, Mizushima M, *et al.* Interstitial pneumonia in Hermansky-Pudlak syndrome: significance of florid foamy swelling/degeneration (giant lamellar body degeneration) of type-2 pneumocytes. *Virchows Arch* 2000;437:304–313.
7. Pierson DM, Ionescu D, Qing G, Yonan AM, Parkinson K, Colby TC, Leslie K. Pulmonary fibrosis in Hermasky-Pudlak Syndrome: a case report and review. *Respiration* 2006;73:382–395.
8. Gahl WA, Brantly M, Troendle J, Avila NA, Padua A, Montalvo C, Cardona H, Calis KA, Gochuico B. Effect of pirfenidone on the pulmonary fibrosis of Hermansky-Pudlak syndrome. *Mol Genet Metab* 2002;76:234–242.
9. Feng L, Rigatti BW, Novak EK, Gorin MB, Swank RT. Genomic structure of the mouse Ap3b1 gene in normal and pearl mice. *Genomics* 2000;69:370–379.
10. Thomas AQ, Lane K, Phillips J III, Prince M, Markin C, Speer M, Schwartz DA, Gaddipati R, Marney A, Johnson J, *et al.* Heterozygosity for a surfactant protein C gene mutation associated with usual interstitial pneumonitis and cellular nonspecific interstitial pneumonitis in one kindred. *Am J Respir Crit Care Med* 2002;165:1322–1328.
11. Nogee LM, Dunbar AE III, Wert SE, Askin F, Hamvas A, Whitsett JA. A mutation in the surfactant protein C gene associated with familial interstitial lung disease. *N Engl J Med* 2001;344:573–579.
12. Bridges JP, Wert SE, Nogee LM, Weaver TE. Expression of a human surfactant protein C mutation associated with interstitial lung disease disrupts lung development in transgenic mice. *J Biol Chem* 2003;278: 52739–52746.
13. Bridges JP, Xu Y, Na CL, Wong HR, Weaver TE. Adaptation and increased susceptibility to infection associated with constitutive expression of misfolded SP-C. *J Cell Biol* 2006;172:395–407.
14. Bullard JE, Wert SE, Whitsett JA, Dean M, Nogee LM. ABCA3 mutations associated with pediatric interstitial lung disease. *Am J Respir Crit Care Med* 2005;172:1026–1031.
15. Shulenin S, Nogee LM, Annilo T, Wert SE, Whitsett JA, Dean M. ABCA3 gene mutations in newborns with fatal surfactant deficiency. *N Engl J Med* 2004;350:1296–1303.
16. Uhal BD, Joshi I, Hughes WF, Ramos C, Pardo A, Selman M. Alveolar epithelial cell death adjacent to underlying myofibroblasts in advanced fibrotic human lung. *Am J Physiol* 1998;275:L1192–L1199.
17. Lawson WE, Polosukhin VV, Stathopoulos GT, Zoia O, Han W, Lane KB, Li B, Donnelly EF, Holburn GE, Lewis KG, *et al.* Increased and prolonged pulmonary fibrosis in surfactant protein C-deficient mice following intratracheal bleomycin. *Am J Pathol* 2005;167:1267–1277.
18. Na C-L, Duan CX, Apsley KS, Weaver TE. Abnormal alveolar type 2 cell phenotype in AP-3 Mutant Mocha and Pearl mice: an electron microscopy study. *Microsc Microanal* 2003;9:1426–1427.
19. Guttentag SH, Akhtar A, Tao JQ, Atochina E, Rusiniak ME, Swank RT, Bates SR. Defective surfactant secretion in a mouse model of Hermansky-Pudlak syndrome. *Am J Respir Cell Mol Biol* 2005;33: 14–21.
20. Lyerla TA, Rusiniak ME, Borchers M, Jahreis G, Tan J, Ohtake P, Novak EK, Swank RT. Aberrant lung structure, composition, and function in a murine model of Hermansky-Pudlak syndrome. *Am J Physiol Lung Cell Mol Physiol* 2003;285:L643–L653.
21. Yoshioka Y, Kumasaka T, Ishidoh K, Kominami E, Mitani K, Hosokawa Y, Fukuchi Y. Inflammatory response and cathepsins in silica-exposed Hermansky-Pudlak syndrome model pale ear mice. *Pathol Int* 2004;54: 322–331.

22. Young LR, Borchers MT, Allen HL, Gibbons RS, McCormack FX. Lung-restricted macrophage activation in the pearl mouse model of hermansky-pudlak syndrome. *J Immunol* 2006;176:4361–4368.
23. Allen HL, Deepe GS Jr. Apoptosis modulates protective immunity to the pathogenic fungus Histoplasma capsulatum. *J Clin Invest* 2005;115: 2875–2885.
24. Teder P, Vandivier RW, Jiang D, Liang J, Cohn L, Pure E, Henson PM, Noble PW. Resolution of lung inflammation by CD44. *Science* 2002;296:155–158.
25. Chen ES, Greenlee BM, Wills-Karp M, Moller DR. Attenuation of lung inflammation and fibrosis in interferon-gamma-deficient mice after intratracheal bleomycin. *Am J Respir Cell Mol Biol* 2001;24:545–555.
26. Moseley PL, Hemken C, Hunninghake GW. Augmentation of fibroblast proliferation by bleomycin. *J Clin Invest* 1986;78:1150–1154.
27. Maeyama T, Kuwano K, Kawasaki M, Kunitake R, Hagimoto N, Hara N. Attenuation of bleomycin-induced pneumopathy in mice by monoclonal antibody to interleukin-12. *Am J Physiol Lung Cell Mol Physiol* 2001;280:L1128–L1137.
28. Daniels CE, Wilkes MC, Edens M, Kottom TJ, Murphy SJ, Limper AH, Leof EB. Imatinib mesylate inhibits the profibrogenic activity of TGF-beta and prevents bleomycin-mediated lung fibrosis. *J Clin Invest* 2004;114:1308–1316.
29. Schrier DJ, Kunkel RG, Phan SH. The role of strain variation in murine bleomycin-induced pulmonary fibrosis. *Am Rev Respir Dis* 1983;127: 63–66.
30. Avila NA, Brantly M, Premkumar A, Huizing M, Dwyer A, Gahl WA. Hermansky-Pudlak syndrome: radiography and CT of the chest compared with pulmonary function tests and genetic studies. *AJR Am J Roentgenol* 2002;179:887–892.
31. Huizing M, Scher CD, Strovel E, Fitzpatrick DL, Hartnell LM, Anikster Y, Gahl WA. Nonsense mutations in ADTB3A cause complete deficiency of the beta3A subunit of adaptor complex-3 and severe Hermansky-Pudlak syndrome type 2. *Pediatr Res* 2002;51:150–158.
32. Shotelersuk V, Dell'Angelica EC, Hartnell L, Bonifacino JS, Gahl WA. A new variant of Hermansky-Pudlak syndrome due to mutations in a gene responsible for vesicle formation. *Am J Med* 2000;108:423–427.
33. Noble PW, Homer RJ. Idiopathic pulmonary fibrosis: new insights into pathogenesis. *Clin Chest Med* 2004;25:749–758. (vii.).
34. Selman M, Pardo A. Idiopathic pulmonary fibrosis: an epithelial/fibroblastic cross-talk disorder. *Respir Res* 2002;3:3.
35. Vassallo R, Thomas CF. Advances in the treatment of rheumatic interstitial lung disease. *Curr Opin Rheumatol* 2004;16:186–191.
36. Cavarra E, Carraro F, Fineschi S, Naldini A, Bartalesi B, Pucci A, Lungarella G. Early response to bleomycin is characterized by different cytokine and cytokine receptor profiles in lungs. *Am J Physiol Lung Cell Mol Physiol* 2004;287:L1186–L1192.
37. Bonniaud P, Margetts PJ, Ask K, Flanders K, Gauldie J, Kolb M. TGF-beta and Smad3 signaling link inflammation to chronic fibrogenesis. *J Immunol* 2005;175:5390–5395.
38. Kelly M, Kolb M, Bonniaud P, Gauldie J. Re-evaluation of fibrogenic cytokines in lung fibrosis. *Curr Pharm Des* 2003;9:39–49.
39. Fichtner-Feigl S, Strober W, Kawakami K, Puri RK, Kitani A. IL-13 signaling through the IL-13alpha2 receptor is involved in induction of TGF-beta1 production and fibrosis. *Nat Med* 2006;12:99–106.
40. Huaux F, Lardot C, Arras M, Delos M, Many MC, Coutelier JP, Buchet JP, Renauld JC, Lison D. Lung fibrosis induced by silica particles in NMRI mice is associated with an upregulation of the p40 subunit of interleukin-12 and Th-2 manifestations. *Am J Respir Cell Mol Biol* 1999;20:561–572.
41. Huaux F, Arras M, Tomasi D, Barbarin V, Delos M, Coutelier JP, Vink A, Phan SH, Renauld JC, Lison D. A profibrotic function of IL-12p40 in experimental pulmonary fibrosis. *J Immunol* 2002;169:2653–2661.
42. Kuwano K, Miyazaki H, Hagimoto N, Kawasaki M, Fujita M, Kunitake R, Kaneko Y, Hara N. The involvement of Fas-Fas ligand pathway in fibrosing lung diseases. *Am J Respir Cell Mol Biol* 1999;20:53–60.
43. Uhal BD. Apoptosis in lung fibrosis and repair. *Chest* 2002;122:293S–298S.
44. Hagimoto N, Kuwano K, Inoshima I, Yoshimi M, Nakamura N, Fujita M, Maeyama T, Hara N. TGF-beta 1 as an enhancer of Fas-mediated apoptosis of lung epithelial cells. *J Immunol* 2002;168:6470–6478.
45. Martin TR, Hagimoto N, Nakamura M, Matute-Bello G. Apoptosis and epithelial injury in the lungs. *Proc Am Thorac Soc* 2005;2:214–220.
46. Kuwano K, Hagimoto N, Kawasaki M, Yatomi T, Nakamura N, Nagata S, Suda T, Kunitake R, Maeyama T, Miyazaki H, *et al.* Essential roles of the Fas-Fas ligand pathway in the development of pulmonary fibrosis. *J Clin Invest* 1999;104:13–19.
47. Kuwano K, Kunitake R, Maeyama T, Hagimoto N, Kawasaki M, Matsuba T, Yoshimi M, Inoshima I, Yoshida K, Hara N. Attenuation of bleomycin-induced pneumopathy in mice by a caspase inhibitor. *Am J Physiol Lung Cell Mol Physiol* 2001;280:L316–L325.
48. Hagimoto N, Kuwano K, Miyazaki H, Kunitake R, Fujita M, Kawasaki M, Kaneko Y, Hara N. Induction of apoptosis and pulmonary fibrosis in mice in response to ligation of Fas antigen. *Am J Respir Cell Mol Biol* 1997;17:272–278.
49. Blott EJ, Bossi G, Clark R, Zvelebil M, Griffiths GM. Fas ligand is targeted to secretory lysosomes via a proline-rich domain in its cytoplasmic tail. *J Cell Sci* 2001;114:2405–2416.
50. Clark RH, Stinchcombe JC, Day A, Blott E, Booth S, Bossi G, Hamblin T, Davies EG, Griffiths GM. Adaptor protein 3-dependent microtubule-mediated movement of lytic granules to the immunological synapse. *Nat Immunol* 2003;4:1111–1120.